Energy partitioning in two kinds of NO molecules generated from the reaction of O (1 D) with N 2 O : Vibrational state distributions of "new" and "old" NO's

Hiroshi Akagi, Yo Fujimura, and Okitsugu Kajimoto

Articles you may be interested in

A crossed beam study of 18O(3P)+NO2 and 18O(1D)+NO2: Isotope exchange and O2+NO formation channels
J. Chem. Phys. **137**, 044302 (2012); 10.1063/1.4736567

Quasiclassical trajectory study of O (D 1) + N 2 O → N O + N O : Classification of reaction paths and vibrational distribution
J. Chem. Phys. **124**, 184315 (2006); 10.1063/1.2191041

Exit interaction effect on nascent product state distribution of O (1 D)+ N 2 O → NO + NO
J. Chem. Phys. **120**, 6430 (2004); 10.1063/1.1649721

Scalar and vector properties of the NO (v ′ =0) produced from the reaction O (1 D)+ N 2 O→NO+NO
J. Chem. Phys. **111**, 592 (1999); 10.1063/1.479340

Ab initio molecular orbital and density functional characterization of the potential energy surface of the N 2 O+Br reaction
J. Chem. Phys. **109**, 9410 (1998); 10.1063/1.477602

Energy partitioning in two kinds of NO molecules generated from the reaction of O(^1D) with N$_2$O: Vibrational state distributions of ''new'' and ''old'' NO's

Hiroshi Akagi, Yo Fujimura, and Okitsugu Kajimoto[a]
Department of Chemistry, Graduate School of Science, Kyoto University, Kitashirakawa-Oiwakecho, Sakyo-ku, Kyoto 606-8502, Japan
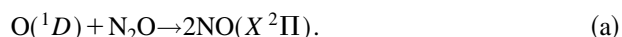
The reaction of O(^1D) with N$_2$O produces two kinds of NO molecules, the ''old'' one which originally exists in N$_2$O and the ''new'' one which includes the attacking O atom. Using the isotopically labeled reagent, we determined the vibrational state distributions of these NO's ($X\,^2\Pi$; $v=0-17$) separately. To obtain the distributions, two types of experiments were performed with the laser-induced fluorescence (LIF) technique via the NO $A\leftarrow X$ and $B\leftarrow X$ transitions. First, the relative populations of NO molecules (the sum of the two kinds of NO's) in $v=0-11$ levels were measured with unlabeled reagents. Then, isotopically labeled reaction, ^{18}O(^1D) $+$N$_2$^{16}O$\rightarrow$N^{18}O$+$N^{16}O, was utilized to determine the relative ratio between the two kinds of NO's in the vibrational levels of $v=0-5$ and 12–15. Combining the above results with previously determined vibrational state distribution of NO in high vibrational levels ($v=11-17$) [J. Chem. Soc., Faraday Trans. **94**, 1575 (1998)], we were able to obtain a complete set of vibrational state distributions. It was found that the old NO dominantly populated in $v=0$ and 1 whereas the new NO extended its population toward higher vibrational levels ($v=4-15$). However, in high vibrational levels, the old NO still have a considerable population due to the rapid energy transfer to the old NO. The observed efficient energy transfer to the old NO is attributed to the absence of light atoms in the present reacting system. Compared with the system including hydrogen atoms, the state density and the momentum coupling among the vibrational modes are much larger and accelerate the energy redistribution in spite of the short lifetime. © *1999 American Institute of Physics.* [S0021-9606(99)02225-4]

I. INTRODUCTION

Nascent internal state distribution of reaction products contains rich information of reaction dynamics on a potential-energy surface (PES) and hence detailed data of the product state distribution have been accumulated for a variety of reactions.[1] However, there are few cases where the internal state distribution of all the reaction products were reported. One such example is the reaction ^{16}O(^1D) $+$H$_2$^{18}O$\rightarrow^{16}$OH$+^{18}$OH.[2] The authors found a completely different state distribution between ^{16}OH and ^{18}OH. This observation clearly indicated that the energy mixing was far from complete even in the reaction having a deep potential well on the PES. Thus, the determination of the state distributions in *all* reaction products is extremely important to deepen the understanding of reaction dynamics on the potential-energy surface.

In the present study, we have determined the vibrational state distribution of all the products of the reaction,

$$O(^1D)+N_2O\rightarrow 2NO(X\,^2\Pi). \qquad (a)$$

This reaction is one of the fundamental reactions in stratospheric chemistry and also a prototype reaction of O(^1D) atoms. The reaction produces two kinds of NO molecules,

that is, a ''new'' NO which contains a reactant O atom and an ''old'' NO which originally exists in the reactant N$_2$O. Isotopically labeled studies of this reaction have been carried out by two groups. Using ^{15}N^{14}NO, Simons and co-workers have observed the overlapped signal of ^{15}NO and ^{14}NO in the lower vibrational levels $v=0-2$ and they reported that the contributions from the ^{15}NO and ^{14}NO signals in the $v=1$ and 2 levels were comparable.[3] Their observation indicates that the vibrational energy is distributed equally between the two NO's. On the other hand, Honma *et al.* performed an *aligned* O(^1D)$+^{15}$N^{14}NO reaction using a ^{15}N^{14}NO dimer formed in a supersonic jet and compared the relative populations of the two kinds of NO's at $v=0$ and 3.[4] They found that the old ^{14}NO was dominant in $v=0$ while the new ^{15}NO was more populated in $v=3$. Based on their experimental results, they have proposed an interpretation that the excess energy is mainly poured into the new ^{15}NO while the old ^{14}NO stays in its low vibrational level.

The reaction (a) occurs almost at every collision with the rate constant of 7.2×10^{-11} cm^3 molecule^{-1} s^{-1},[5] and has a large exothermicity $\Delta H^0(0)=-342.6$ kJ mol^{-1},[6] which can excite the product NO up to $v=16$. In contrast to the large exothermicity, the bond dissociation energy of (NO)$_2$, a possible intermediate of this reaction, is very small ($D_0\approx700$ cm^{-1}).[7] Therefore, the well of PES, if any, must be extremely shallow. According to the *ab initio* MO calcula-

---

[a]Author to whom correspondence should be addressed.

tions, this reaction has a significantly attractive PES, on which the heat of reaction is mainly released during the approach of the O atom toward N_2O.[8] Under such a situation, the trajectories running on the PES quickly pass through the interactive region, where the four atoms can interact with each other, and the lifetime of a collision complex must be quite short. Consequently, incomplete vibrational energy redistribution within the collision complex is expected. These considerations suggest that most of the available energy is given to the newly formed NO, with a possibility of inverted vibrational state distribution. On the other hand, the old NO acts as a spectator and remains vibrationally cold. As a result, the vibrational state distribution of NO in the unlabeled reaction could be bimodal, corresponding to the distribution of each NO molecules. In order to check the above expectation and obtain more detailed information of the reaction dynamics, we have determined the complete vibrational energy distributions of the two NO molecules.

According to the previous studies on the unlabeled reaction, the vibrational state distribution in lower vibrational levels ($v = 0 - 4$) looks statistical.[3] In our previous work detecting the highly vibrationally excited NO($v = 11 - 17$), the vibrational population gradually declines as the vibrational quantum number increases without any indication of inverted population, and it is even slightly colder than the statistical distribution.[9] Brouard *et al.* have determined the rotational and translational state distributions in detail,[10] and concluded that there are two types of reaction dynamics. A direct stripping reaction yields NO($v = 0$) and NO($v = 16 - 18$) whereas an indirect process, in which the collision complex survives for a sufficient time to allow extensive rovibrational energy redistribution, leads to the formation of rotationally excited NO products in $v = 1 - 15$.

The present work aims at determining the complete set of the vibrational state distributions of product NO's generated from the isotopically labeled reaction,

$$^{18}O(^1D) + N_2{}^{16}O \rightarrow N^{18}O + N^{16}O. \qquad (a')$$
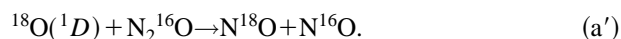
For this purpose, we carried out two types of experiments utilizing the LIF technique. First, we measured the vibrational state distribution of total NO produced from the unlabeled $^{16}O(^1D) + N_2{}^{16}O$ reaction. Then, using isotopically labeled reaction, we determined the relative populations between the old $N^{16}O$ and the new $N^{18}O$ in each vibrational level. These two types of experiments bring the ''complete'' vibrational state distributions. Although the experimental and analytical procedures are almost the same as our previous work,[9] the LIF detection with the $A \leftarrow X$ transition was utilized in this experiment in addition to the previously used $B \leftarrow X$ transition. The quenching rate coefficient of NO(A) by N_2O, O_3, and O_2 were also determined in this study in order to deduce reliable vibrational populations.

II. EXPERIMENT

Since the experimental procedure used in the present experiments is similar to the previous one,[9] the experimental apparatus and procedure are described briefly. O(^1D) and $^{18}O(^1D)$ atoms were generated by the O_3 and $^{18}O_3$ photodissociations at 266 nm, respectively. The kinetic energies of

the $^{16}O(^1D)$ and $^{18}O(^1D)$ atoms, together with the heat of reaction, provide the total available energies of 364.2 and 363.5 kJ mol^{-1}, respectively,[11] and can excite $N^{16}O$ and $N^{18}O$ up to $v = 18$ and 19, respectively. N_2O and O_3 (or $^{18}O_3$) gases were introduced into a reaction cell, a glass bulb of 24 cm diam, up to 1 Torr. Partial pressures of N_2O and O_3 were 900 and 100 mTorr, respectively. O_3 and $^{18}O_3$ were synthesized by the silent discharge technique[12] from O_2 (Teisan 99.995%) and $^{18}O_2$ (Matheson 99.2 at %), respectively. Because $^{18}O_2$ gas is costly and easily consumed in the flow system, all experiments were carried out under static conditions. N_2O (Showa-Denko 99.999%) was used without further purification.

The O(^1D) + N_2O reaction was initiated by O_3 photolysis at 266 nm, with a frequency-quadrupled Nd:YAG laser (Quanta Ray DCR-11). The reaction product NO was detected with a LIF technique by using the NO $A\,{}^2\Sigma^+(v = 0 - 2) \leftarrow X\,{}^2\Pi(v = 0 - 11)$ and $B\,{}^2\Pi(v = 0 - 2) \leftarrow X\,{}^2\Pi(v = 12 - 15)$ transitions. For the LIF detection, three types of light sources were used. For the wavelength shorter than 290 nm, a frequency doubled output (Inrad Autotracker-III AT-III) of a dye laser (LAS LDL20505) pumped by the third harmonics of a Nd:YAG laser (Quanta Ray GCR-4) was used. The dye laser was pumped by the second harmonics of the Nd:YAG laser for the light $290 < \lambda < 370$ nm. The light of the third region $\lambda > 370$ nm was obtained by pumping a dye laser (Lambda Physik LPD 100) with a XeCl excimer laser (Lambda Physik LPX 3000). The intensity of the probe laser light was attenuated in order to avoid saturation in absorption. The delay time between the photolysis and the probe laser lights was 5 μs. All systems were operated with a repetition rate of 10 Hz.

To determined the relative vibrational distribution among $v = 0$, 1, 3, 6, 9, and 11 vibrational levels, we compared the relative intensity of the two transitions originating from different ground vibrational levels. When a single dye covers the wavelength range of the two transitions from different vibrational levels, it is easy to estimate the relative population for these two vibrational levels. This was not the case for measuring the relative populations between $v = 1$ and 3, and between $v = 9$ and 11. For these vibrational levels, we have to change dye solutions for a set of experiments, which often deflect the laser path away, and consequently, the laser power monitored at the cell entrance might not coincide with the power at the center of the reaction cell. To avoid this discrepancy, we monitored the laser power at the cell exit using a joulemeter (Gentec ED-100A) with a wide surface. The detailed procedures for calculating the real population from the observed intensity were described in detail in the previous paper.[9]

III. ANALYSIS

In the previous study, we have carefully assessed several factors which prevent us from accurate determination of the vibrational population, and carried out the necessary corrections.[9] Since the corrections are almost the same for the present study, only a brief description will be given in the following sections with a due stress on the new corrections.

J. Chem. Phys., Vol. 111, No. 1, 1 July 1999

Energy partition reaction of O(^1D) with N$_2$O   117

A. Corrections for the decrease of O$_3$ concentration

Because the present experiments are performed in a bulb under static conditions, the composition of the reaction gas mixture gradually varies as the photolysis proceeds. In particular the decrease of O$_3$ concentration requires the following corrections:

(1) Decrease in the amount of O(^1D) atoms generated from O$_3$ photodissociation.
(2) Increase in the fraction of O(^1D) reacting with N$_2$O.
(3) Decrease in the absorption of fluorescence from NO(A,B) by O$_3$.
(4) Decrease in the rate of NO(A,B) quenching by component gases.
(5) Decrease in the absorption of probe laser light by O$_3$.

Since the $A \leftarrow X$ transition is utilized for the LIF detection in the present experiments, the third and fourth effects are more serious than in the previous study. Furthermore, when NO molecules in the lower vibrational levels ($v = 0-6$) are monitored with the $A \leftarrow X$ transitions, the wavelengths of the probe laser light overlaps with the Hartley band of O$_3$ (200–320 nm), whose absorption coefficients are quite large.[5,12,13] We should, then, estimate the probe laser intensity at the center of reaction cell to correct for the signal intensities. For the three corrections, 3–5, the detailed procedures are described below.

1. Absorption of the NO(A) fluorescence by O$_3$

Because of the large absorption cross-section of O$_3$ at Hartley band, ca. 8%–26% of the fluorescence from the NO(A) in $v = 0-2$ is absorbed by 100 mTorr O$_3$ during the passage from the center to the detection window of the reaction cell. To obtain the reliable relative populations among different vibrational levels of NO(A), experimental data must be corrected for this O$_3$ absorption. The procedure used previously for NO(B) was adopted for this correction except for using the transition wavelength $\lambda_{v'v''}$ and the transition probability $R_{v'v''}$ of NO(A).[14] To apply Eq. (IX) in Ref. 9 to the correction, we measured the O$_3$ absorbance at 266 nm from the intensities of photolysis laser light before and after passing through the reaction cell.

2. Rates of NO(A) quenching by buffer gases

In the previous work using NO $B \leftarrow X$ transition for the LIF detection,[9] we have measured the fluorescence decay rates of NO(B) in $v = 0-3$, and determined the quenching rate constants of NO(B) by O$_3$, N$_2$O, O$_2$, and N$_2$ in order to correct the LIF intensity for the loss of NO(B). Since A state fluorescence was used for the LIF detection in the present experiments, we should correct for the quenching of NO(A) by the component gases in the reaction cell. The quenching processes by O$_3$, N$_2$O, and O$_2$ could be significant, since these gases are abundant in the cell. The quenching rate constants of NO(A) in $v = 0$ by N$_2$O (Refs. 15 and 16) and O$_2$ (Refs. 15–18) and in $v = 1$ by O$_2$ (Ref. 18) have already been reported, and all of these processes are found to be completed in almost a single collision efficiency. This large quenching efficiency must seriously affect the evaluation of the vibrational population by the LIF measurements. Since

TABLE I. Rate constants for the quenching of NO($A\ ^2\Sigma^+$; $v = 0-2$) by O$_3$, N$_2$O, and O$_2$.[a]

	k_q of NO($A\ ^2\Sigma^+$)/10^{-12} cm^3 molecule^{-1} s^{-1}		
Quencher	0	1	2
O$_3$	573±57 [−]	450±45 [−]	781±78 [−]
N$_2$O	471±47 [506±33][c]	499±50 [−]	466±47 [−]
O$_2$	151±15 [162±5][c]	160±16 [140±13][d]	149±15 [−]
Radiative rate[b] /10^5 s^{-1}	49.5±3.7	52.1±4.1	54.9±3.2

[a]The experimental uncertainty corresponds to 1σ in the least-squares fit.
[b]Reference 14.
[c]Reference 16.
[d]Reference 18.

the information of other rate constants was not available, we have determined the quenching rate constants of NO(A) in $v = 0-2$ by measuring the lifetimes at five different gas compositions. Using the obtained lifetimes of NO(A; $v = 0-2$), we have evaluated the absolute rate constants based on the most recently reported quenching constants of NO(A; $v = 0$) by N$_2$O and O$_2$.[16] We have assumed that the relative rate constants between N$_2$O and O$_2$ are not dependent on the vibrational level. The results obtained for each vibrational level of NO(A) are listed in Table I, together with the radiative rates used in this analysis.[14] The quenching rate constants are compared with the available data, showing a good agreement. These values were used to estimate the loss of the NO(A) fluorescence by the quenching processes.

3. Absorption of the probe laser light by O$_3$

Ozone gases significantly absorbs the probe laser light used for the detection of NO's in $v = 0-6$ levels; the wavelengths of probe laser are in the O$_3$ Hartley band. In a typical case, the probe laser intensity at 256 nm is reduced to the two-thirds of the incident light by the time it reaches the center of the cell.[5] Using the Lambert–Beer's law, we can estimate the probe laser intensity at the center of reaction cell as

$$I_{\text{center}}^{\text{probe}} = I_{\text{in}}^{\text{probe}} \exp[-k(\lambda_{v'v'};O_3)[O_3]l_{\text{cell}}/2] \quad (1)$$

$$= I_{\text{in}}^{\text{probe}} \exp\left[-\frac{k(\lambda_{v'v''};O_3)}{2k(266\ \text{nm};O_3)}\ln\left(\frac{I_{\text{in}}}{I_{\text{out}}}\right)\right] \quad (2)$$

$$= I_{\text{in}}^{\text{probe}}\left(\frac{I_{\text{out}}}{I_{\text{in}}}\right)^{k(\lambda_{v'v''};O_3)/2k(266\ \text{nm};O_3)}, \quad (3)$$

where $I_{\text{in}}^{\text{probe}}$ is the intensity of probe laser light at the cell entrance, $k(\lambda_{v'v''};O_3)$ is the O$_3$ absorption coefficient at a wavelength $\lambda_{v'v''}$, [O$_3$] is the O$_3$ concentration, and l_{cell} is the path length of the photolysis laser light in the reaction cell, respectively. In the derivation Eq. (2) from Eq. (1), we substitute Eq. (I) of Ref. 9 into [O$_3$]. Equation (3), together with experimentally obtained value of $I_{\text{out}}/I_{\text{in}}$, was used for the correction of the signal intensities.

B. Possibility of vibrational relaxation and vibrational energy transfer between two NO's

Since the present experiment were carried out under medium pressure and long delay conditions, we should consider vibrational quenching of product NO. In our previous paper, we mentioned that the vibrational quenching had no significant effect for high vibrational levels ($v = 11$–17).[9] In the lower vibrational states, the vibrational quenching rate constants for NO ($v = 1$–11) colliding with N_2O (Ref. 19) and those for NO ($v = 1$–7) colliding with O_2 (Ref. 20) have already been known. According to the available information, the fraction of vibrationally quenched NO is calculated to be less than 2% at 5 μs after the photolysis. However, the quenching rate constant by O_3 which is the highly abundant component in the gas mixture, has not yet been reported to our best knowledge. Thus, we made a comparison between signal intensities under the conditions of different O_3 partial pressures. We did not find any changes in $v = 1$–11, and therefore neglected the vibrational quenching of NO by the component gases including O_3.

In addition to the vibrational quenching, vibrational energy transfer between $N^{16}O$ and $N^{18}O$ should be considered since this effect is expected to equalize the populations of the two NO's in each vibrational level by scrambling the nascent populations. However, this had little influence, because the partial pressures of $N^{16}O$ and $N^{18}O$ in the reaction cell were negligibly small and they were quickly consumed by the efficient reaction

$$NO + O_3 \rightarrow NO_2 + O_2$$
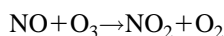
$$(k_{298} = 1.8 \times 10^{-14} \ cm^3 \, molecule^{-1} \, s^{-1})^5, \tag{b}$$

and all NO molecules disappeared before the next shot of the photolysis laser. To ascertain that the vibrational energy transfer does not produce any serious effect on the population ratio between two NO's, we performed an additional experiments with shorter (3 μs) and longer (7 μs) delay times for $v = 4$, 14, and 15 levels. The relative populations evaluated from these three sets of data did not showed any difference within the experimental error, which confirmed the negligible influence by the energy transfer.

C. Determination of vibrational state distribution or relative populations between NO's

In order to determine the vibrational state distribution or the population ratio between $N^{16}O$ and $N^{18}O$, we need to obtain the rotational state distribution in each vibrational level with high accuracy. Since the extremely high rotational excitation of the NO molecules produced from this reaction prevents us from the accurate determination of rotational distribution, we performed the experiments under medium pressure (1 Torr) and long delay time (5 μs) conditions. Under such conditions, product NO molecules can collide with other buffer gases about 100 times before the detection. Thus, rotationally excited NO molecules are fully relaxed to the thermal distribution, whereas the vibrational population remains the same as nascent. The experiments showed that the rotational distribution can well be described by a single Boltzmann temperature around 300 K.
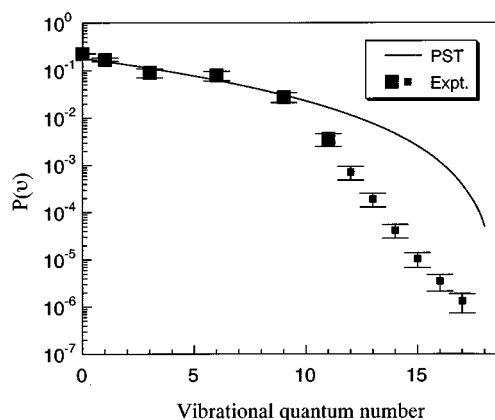

FIG. 1. Vibrational state distribution of NO($X\,^2\Pi$) generated from the O(^1D)+N_2O reaction. The large and small square symbols mean the present results and those calculated from the data in Ref. 9, respectively. The solid line shows the distribution predicted from the phase space theory. The given experimental uncertainty corresponds to 1σ in the least-squares fit.

Once we know the accurate rotational temperature for each vibrational level under the rotationally relaxed condition, the measurement of only one rovibrational peak of a given vibrational level is enough to estimate the total population of the vibrational level (i.e., the sum of all rotational levels). For the actual experiments, the intensities of more than three rovibrational peaks were selected in each band and their intensities were measured. To determine the population ratio between two different vibrational levels, the intensities of the selected peaks in the two corresponding bands were measured *within a single scan*. This measurements were performed three times for each pair of vibrational levels. A statistical analysis for the results of these measurements was made to evaluate the population ratio.

IV. RESULTS

A. Vibrational state distribution of *total* NO products generated from $^{16}O(^1D)$+$N_2{}^{16}O$

To extend the previously obtained vibrational state distribution of highly excited NO ($v = 11$–17) (Ref. 9) to the lower vibrational levels ($v = 0$–11), we determined the relative vibrational distribution among $v = 0$, 1, 3, 6, 9, and 11 vibrational levels and estimated the vibrational populations of in-between levels by interpolation.

The vibrational state distribution thus obtained is shown in Fig. 1, together with the previous results for $v = 11$–17. As a whole, the vibrational population declines as the vibrational quantum number increases. In Fig. 1, we also plotted the distribution predicted from phase space theory (PST).[21] The experimental populations between $v = 0$ and 9 agree closely with the PST distribution, whereas the population above $v = 9$ rapidly decreases with increasing vibrational quantum number and the distribution is apparently colder than the statistical one. From this distribution, we could estimate the average vibrational energy $\langle E_{vib}\rangle$ by assuming that the vibrational population changes smoothly. The obtained value, 5500 cm^{-1}, is comparable to that predicted from the PST distribution, 6400 cm^{-1}. The discrepancy in the high
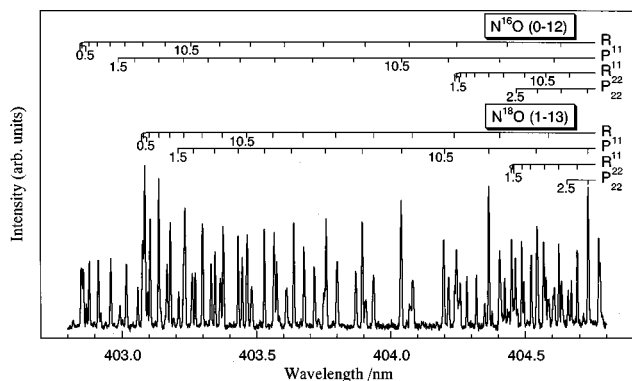
FIG. 2. Rotationally relaxed LIF spectrum of N^{16}O($v=12$) and N^{18}O($v=13$) produced from the ^{18}O(^1D)+N$_2$^{16}O reaction. The transitions correspond to N^{16}O $B\leftarrow X(0\leftarrow 12)$ and N^{18}O $B\leftarrow X(1\leftarrow 13)$. Spectrum was taken with 5 μs delay time and 1 Torr total pressure. Since the transition probability of the $B\leftarrow X(1\leftarrow 13)$ is approximately 2.4 times larger than that of the $B\leftarrow X(0\leftarrow 12)$, the population of the old NO in $v=12$ level is almost the same as that of the new NO in $v=13$ level.

vibrational levels ($v=9$–17) has little influence on the average vibrational energies, because of the minor populations in these levels.

Simons and coworkers have reported that the vibrational distribution in $v=0$–4 is described by a Boltzmann-type function with a vibrational temperature $T_{vib}\approx 6000$K.[3] However, the distribution in $v=0$–17 determined by our experiments could not be described by a single Boltzmann distribution. If we fit the distributions in $v=0$–9 and 9–17 ranges separately with different single exponential functions, the temperatures are $\approx$ 12 000 and 2 000 K, respectively. The discrepancy in the vibrational temperature between the two groups may arise from vibrational relaxation, since Simons' group performed the experiments under higher pressures (40 Torr). Recently, Wang et al. have determined the vibrational state distribution in $v=1$–11 and reported that the distribution is characterized by a single Boltzmann temperature $T_{vib}\approx 9000$ K.[22] This figure is in satisfactory agreement with our result for the lower vibrational levels.

B. Relative populations between N^{18}O and N^{16}O generated from ^{18}O(^1D)+N$_2$^{16}O

Using ^{18}O$_3$, we have determined the relative populations between the new N^{18}O and the old N^{16}O in both the lower ($v=0$–5) and higher ($v=12$–15) levels. The LIF spectrum containing the N^{18}O $B\leftarrow X(1\leftarrow 13)$ and N^{16}O $B\leftarrow X(0\leftarrow 12)$ transitions is shown in Fig. 2. Each spectrum was obtained in the rotationally relaxed conditions. For the assignment of N^{18}O peaks, we utilized the rotational constants which were obtained from the rotational constants[23] of N^{16}O multiplied by the isotope factor, $\rho=\sqrt{\mu(\mathrm{N}^{16}\mathrm{O})/\mu(\mathrm{N}^{18}\mathrm{O})}$ $=0.973\,66$, where $\mu(\mathrm{N}^{16}\mathrm{O})$ and $\mu(\mathrm{N}^{18}\mathrm{O})$ are the reduced masses of N^{16}O and N^{18}O, respectively. These rotational constants of N^{18}O well reproduced the obtained spectra. It should be noted for the isotopically labeled reaction that the vibrational-energy levels of N^{18}O is slightly different from those of N^{16}O, since the vibrational and rotational quanta are different due to the different reduced masses. For example, the vibrational energy of N^{16}O molecule in $v=17$ level is

28 077 cm^{-1}, whereas that of N^{18}O is 27 449 cm^{-1}. The energy difference (628 cm^{-1}) is, however, smaller than a half of the vibrational quantum at $v=16$ of N^{18}O (1400 cm^{-1}). Thus, the difference in the vibrational-energy levels between the isotopically different NO's has very little influence.

The obtained population ratios between N^{18}O and N^{16}O, $N(\mathrm{N}^{18}\mathrm{O};v)/N(\mathrm{N}^{16}\mathrm{O};v)$, are listed in Table II, together with the vibrational state distribution of NO produced from the unlabeled reaction. The listed data clearly shows that old N^{16}O exceeds the new N^{18}O in the lower vibrational levels ($v=0$ and 1), whereas the new N^{18}O becomes the major component above $v=4$. The average vibrational energies of new and old NO's are calculated to $\approx$7000 and 4000 cm^{-1}, respectively. These results coincide with the expectation that the newly formed NO is vibrationally excited and the NO already existing in N$_2$O is vibrationally cold.

It is noteworthy, however, that the amount of energy gained by the old NO is more than what we expected from a simple consideration. Actually, the old NO has a considerable population even in $v=12$–15, which amounts to be 1/3–1/5 population of the new NO. This fact is also apparent from Fig. 2. Since the transition probability of the $B\leftarrow X(1\leftarrow 13)$ for N^{18}O is approximately 2.4 times larger than that of the $B\leftarrow X(0\leftarrow 12)$ used for N^{16}O,[24] this spectrum implies that the population of the old NO in $v=12$ level is almost the same as that of the new NO in $v=13$.

V. DISCUSSION

The vibrational energy distributions of the new and old NO's obtained for the O(^1D)+N$_2$O$\rightarrow$2NO reaction in the present experiment indicate that the new NO is vibrationally more excited than the old NO. The old NO shows its maximum at $v=0$ whereas the population in the new NO has a broad maximum between $v=1$–6. The average vibrational energy of the old NO is 4000 cm^{-1}, which is much smaller than that of the new NO, 7000 cm^{-1}. This trend is understandable because at the initial stage of forming the new NO all the exothermic energy may be located at the O*–N–N part of the collision complex. The localized exothermic energy is gradually transferred into the old NO as the reaction proceeds. This energy mixing process, however, competes with the fission of the N–N bond to form the two NO's. The old NO, therefore, has less chance of accepting the vibrational energy when the lifetime of the collision complex is short.

However, if having observed all the vibrational levels indicated in Fig. 3, one may have another impression that the vibrational energy distributions in the two NO's are rather similar except for the lower levels. In the higher vibrational levels of $v=12$–15, the old NO is produced as many as one-fourth of the new NO. In contrast to the extreme case where all the vibrational excitation is limited to the new NO and the old NO act as a mere spectator, the obtained result indicates that the partitioning of the available energy between the two NO's occurs to a considerable extent. This fact implies that the energy mixing actually occurs between the collisional encounter and the departure of the two NO

TABLE II. Vibrational state distributions of N ^{18}O, N ^{16}O, and the sum of NO's produced from the O(^1D) + N$_2$O reactions.[a,b]

v	$P(\text{N }^{18}\text{O}+\text{N }^{16}\text{O}, v)$	$N(\text{N }^{18}\text{O}; v)/N(\text{N }^{16}\text{O}; v)$	$P(\text{N }^{18}\text{O}, v)/2$[c]	$P(\text{N }^{16}\text{O}; v)/2$[c]
0	0.23	0.30±0.03	0.053	0.17
1	0.17±0.01	0.62±0.13	0.065	0.11
2	(0.11)	1.0±0.1	0.057	0.057
3	0.090±0.019	1.0±0.1	0.046	0.044
4	(0.084)	1.6±0.1	0.052	0.032
5	(0.082)	1.8±0.1	0.052	0.030
6	0.078±0.018	(2.2)	0.054	0.024
7	(0.064)	(2.9)	0.047	0.017
8	(0.046)	(3.4)	0.035	0.010
9	0.027±0.006	(4.3)	0.022	0.0051
10	(0.012)	(4.5)	0.010	0.0022
11	0.0035±0.0011	(3.6)	0.0028	0.00077
12	0.00071±0.00023[e]	2.9±0.2	0.00053	0.00018
13	0.00019±0.00006[e]	4.3±0.3	0.00015	0.000036
14	0.000042±0.000013[e]	[5.2±0.6][d]	0.000035	0.0000067
15	0.000010±0.000004[e]	3.0±0.3	0.0000077	0.0000026
16	0.0000035±0.0000013[e]	(4.0)	0.0000028	0.00000069
17	0.0000013±0.0000006[e]	(4.0)	0.0000010	0.00000026
18	≤0.0000009[e]	...	...	...

[a]Those values given in parentheses are interpolated data.
[b]The experimental uncertainty corresponds to 1σ in the least-squares fit.
[c]These data are calculated from the data included the interpolated values.
[d]This value may be overestimated, because the Franck–Condon factor of the $B-X(1-14)$ for N ^{16}O is almost 10 times larger than that of the $B-X(0-14)$ used for N ^{18}O (Ref. 24).
[e]Those values are calculated from the results in Ref. 9.

molecules and the observed vibrational distribution shows an intermediate features between the complete spectator and the fully statistical cases.

The degree of energy randomization essentially depends on the three factors, the coupling among vibrational modes, the state density at a given energy, and the time for the mixing (the duration of the collisional interaction in the present case). That is, the large coupling, high state density, and the long lifetime of the collision complex enhance the energy randomization. Quantitatively, we can use an analogy between the energy mixing within a collision complex and the intramolecular vibrational-energy redistribution (IVR) within a stable molecule. The rate of IVR for large molecules in the statistical limit is considered to be proportional to the square of the effective coupling v^2 and the state density ρ as,[25]

$$k = \frac{2\pi v^2 \rho}{\hbar}. \tag{4}$$

Since the collision complex has a certain lifetime, we have to take the mixing time into account. When the lifetime of the collision complex is extremely short, the energy mixing can not be achieved even though the IVR rate is quite large.

Concerning the present reaction, O(^1D) + N$_2$O → 2NO, the lifetime of the collision complex is expected to be short, since the potential well for the O–N–N–O intermediate is extremely shallow comparing with the exothermicity of the reaction. The vector correlation data for this reaction obtained in our laboratory[26] suggest that the lifetime is not more than one rotational period. Therefore, the observed mixing of the vibrational energy between the two NO in the present experiments indicates the rapidness of the IVR rate within the collision complex. The reasons for the rapid IVR are discussed in the following sections based on the two main features of the present reaction, that is, the production of the same NO species and the participation of the heavy atoms as compared with the reaction like O(^1D) + H$_2$O → 2OH.

FIG. 3. A complete set of vibrational state distributions of NO($v = 0-17$) produced from the reaction of O(^1D) with N$_2$O. The closed and open triangles depict the populations calculated from the measured and interpolated ratios $N(\text{N}^{18}\text{O})/N(\text{N}^{16}\text{O})$, respectively. The sum distribution is shown by the solid line. The small open circles indicate the population of NO obtained from the unlabeled reaction.

A. Production of two NO molecules

The production of two identical NO species is a unique feature of the present reaction and must give a noticeable influence on the energy mixing. Among the three factors stated above, the state density is strongly affected by the
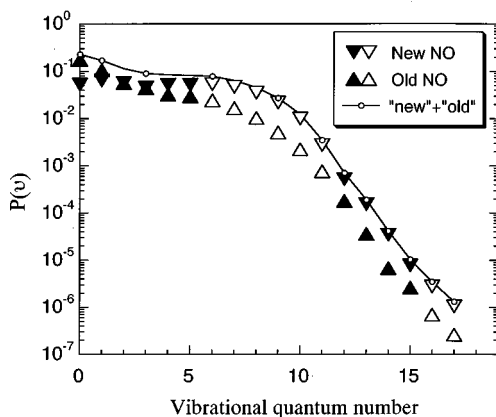
vibrational frequencies of the available vibrational modes. When the identical moieties participate in the IVR process, the presence of completely identical vibrational energy levels considerably enhances the state density at certain energy regions. For example, a bunch of energy levels including the NO stretching vibrations ($v_{new\ NO} + v_{old\ NO} = 17$) appears near the threshold energy and accelerates the energy transfer between the two NO molecules. In terms of the perturbation theory, the process including two nearly identical energy states is estimated to be quite large because the denominator of the perturbation equation is the energy difference of the relevant states and becomes nearly zero. This is called the resonance effect and corresponds to the enhancement of the state density in the expression like the Fermi's Golden Rule.

The above situation is almost the same for the isotopically labeled reaction, $^{18}O(^1D) + N_2^{16}O \rightarrow N^{18}O + N^{16}O$. Although the vibrational frequencies are not strictly the same due to the difference in the mass of oxygen, the two vibrational frequencies of NO's are very similar. The rapid IVR expected in the present experiment can be partly attributed to the resonance effect.

B. Absence of light atoms in the reaction intermediate

An analogous reaction, $O(^1D) + H_2O \rightarrow 2OH$, produces two OH radicals which possess completely different vibrational energy distribution; the new OH is highly excited whereas the old one is quite cold just like a spectator.[2] In view of the resonance effect mentioned above, the two identical OH moieties must enhance the IVR and could give a vibrational distribution similar to the NO molecules in $O(^1D) + N_2O \rightarrow 2NO$. Then, we have to seek the reason for the observed difference between the vibrational energy distributions of these two reactions. The essential difference between these two reactions lies in the weight of atoms constituting the reaction system; the $O(^1D) + H_2O$ reaction contains light hydrogen atoms whereas only the heavy atoms form the reaction system, $O(^1D) + N_2O$. Such difference in their character certainly affects the size of coupling and the state density.

In the case of molecules composed of only heavy atoms, the coupling between the vibrational levels is expected to be much larger than the molecules including light atoms, because the size of momentum (G-matrix) coupling is significantly larger. A comparison between C_2H_2 and C_2D_2 provides the best example. In the case of C_2H_2 molecule, the coupling between the two C–H vibrational modes is small due to the small momentum coupling and the energy levels of these vibrations are well described by a two-parameter local-mode expansion. On the other hand, the deuterating to C_2D_2 increases the momentum coupling and the normal mode expression becomes more appropriate.[27] For acetylene-type molecules Y–X–X–Y, the size of the momentum coupling between two X–Y vibrations is mainly controlled by the masses of the terminal Y atoms. In the same way, the momentum coupling between the two N–O vibrations in the O–N–N–O intermediate is expected to be much larger than in H–O–O–H. The IVR between them, therefore, occurs more efficiently in the collision complex of the $O(^1D)$

$+N_2O$ reaction, making the two vibrational distributions more alike than in the HOOH case.

The state density must be also large for the collision complex containing only heavy atoms. When the molecular size is the same, the vibrational frequencies are smaller for the molecules consisting of heavy atoms than those with light atoms. In the present case, very low vibrational frequencies are reported for a possible intermediate, $(NO)_2$: ν_2(symmetric ONN bending)$=239.4\ cm^{-1}$, ν_3(N–N stretching)$=134.5\ cm^{-1}$, ν_4(torsion)$=117\ cm^{-1}$, and ν_6(antisymmetric bending)$=429.1\ cm^{-1}$.[28] Thus, there is no doubt that the state density in the highly excited level of the collision complex is extremely high in the $O(^1D) + N_2O$ reaction as compared with in the $O(^1D) + H_2O$ reaction.

As mentioned above, the heavy mass effect contributes to the acceleration of IVR in two ways, one through the momentum coupling and the other through the state density. Then, we want to compare the significance of such mass effect with the resonance effect described in the preceding section. Although the resonance effect can contribute both the reactions $O(^1D) + N_2O$ and $O(^1D) + H_2O$, the observed vibrational distributions indicate that the energy partitioning between the two identical products is more enhanced in the case of $O(^1D) + N_2O$. This fact implies that the mass effect plays the major role comparing with the resonance effect. To further elucidate the relative importance between the mass and the resonance effects, we have performed the experiment for the $S(^1D) + N_2O \rightarrow NS + NO$ reaction, which lacks the symmetry and hence the resonance effect. The results confirm the primary importance of the mass effect in the energy randomization within the collision complex.[29]

ACKNOWLEDGMENTS

[1] R. D. Levine and R. B. Bernstein, *Molecular Reaction Dynamics and Chemical Reactivity* (Oxford University Press, New York, 1987).

[2] J. E. Butler, L. D. Talley, G. K. Smith, and M. C. Lin, J. Chem. Phys. **74**, 4501 (1981); K.-H. Gericke, F. J. Comes, and R. D. Levine, *ibid.* **74**, 6106 (1981); F. J. Comes, K.-H. Gericke, and J. Manz, *ibid.* **75**, 2853 (1981); C. B. Cleveland and J. R. Wiesenfeld, *ibid.* **96**, 248 (1992); D. G. Sauder, J. C. Stephenson, D. S. King, and M. P. Casassa, *ibid.* **97**, 952 (1992); D. S. King, D. G. Sauder, and M. P. Casassa, *ibid.* **97**, 5919 (1992); N. Tanaka, M. Takayanagi, and I. Hanazaki, Chem. Phys. Lett. **254**, 40 (1996).

[3] C. R. Boxall, J. P. Simons, and P. W. Tasker, Faraday Discuss. Chem. Soc. **53**, 182 (1972); G. A. Chamberlain and J. P. Simons, J. Chem. Soc., Faraday Trans. 2 **71**, 402 (1975).

[4] K. Honma, Y. Fujimura, and O. Kajimoto, J. Chem. Phys. **88**, 4739 (1988).

[5] R. Atkinson, D. L. Baulch, R. A. Cox, R. F. Hampson, Jr., J. A. Kerr, and J. Troe, J. Phys. Chem. Ref. Data **21**, 1125 (1992).

[6] M. W. Chase, Jr., C. A. Davies, J. R. Downey, Jr., D. J. Frurip, R. A. McDonald, and A. N. Syverud, JANAF *Thermochemical Tables, 3rd ed.,* J. Phys. Chem. Ref. Data Suppl. **14**, 1 (1985).

[7] M. P. Casassa, J. C. Stephenson, and D. S. King, J. Chem. Phys. **89**, 1966 (1988); J. R. Hetzler, M. P. Casassa, and D. S. King, J. Phys. Chem. **95**, 8086 (1991); B. J. Howard and A. R. W. McKellar, Mol. Phys. **78**, 55 (1993); A. Dkhissi, P. Soulard, A. Perrin, and N. Lacome, J. Mol. Spectrosc. **183**, 12 (1997).

[8] I. Last, A. Aguilar, R. Sayós, M. González, and M. Gilibert, J. Phys. Chem. A **101**, 1206 (1997).

[9] H. Akagi, Y. Fujimura, and O. Kajimoto, J. Chem. Soc., Faraday Trans. **94**, 1575 (1998).

[10] F. Green, G. Hancock, A. J. Orr-Ewing, M. Brouard, S. P. Duxon, P. A. Enriquez, R. Sayos, and J. P. Simons, Chem. Phys. Lett. **182**, 568 (1991); M. Brouard, S. P. Duxon, P. A. Enriquez, R. Sayos, and J. P. Simons, J. Phys. Chem. **95**, 8169 (1991); M. Brouard, S. P. Duxon, P. A. Enriquez, and J. P. Simons, J. Chem. Phys. **97**, 7414 (1992).

[11] R. K. Sparks, L. R. Carlson, K. Shobatake, M. L. Kowalczyk, and Y. T. Lee, J. Chem. Phys. **72**, 1401 (1980).

[12] M. Griggs, J. Chem. Phys. **49**, 857 (1968).

[13] H. Okabe, *Photochemistry of Small Molecules* (Wiley, New York, 1978), pp. 237–244.

[14] L. G. Piper and L. M. Cowles, J. Chem. Phys. **85**, 2419 (1986).

[15] I. M. Campbell and R. S. Mason, J. Photochem. **8**, 321 (1978); G. D. Greenblatt and A. R. Ravishankara, Chem. Phys. Lett. **136**, 501 (1987).

[16] P. H. Paul, J. A. Gray, J. L. Durant, Jr., and J. W. Thoman, Jr., Chem. Phys. Lett. **259**, 508 (1996).

[17] I. S. McDermid and J. B. Laudenslager, J. Quant. Spectrosc. Radiat. Transf. **27**, 483 (1982); G. A. Raiche and D. R. Crosley, J. Chem. Phys. **92**, 5211 (1990); M. C. Drake and J. W. Ratcliffe, *ibid.* **98**, 3850 (1993); R. Zhang and D. R. Crosley, *ibid.* **102**, 7418 (1995).

[18] M. Asscher and Y. Haas, J. Chem. Phys. **76**, 2115 (1982).

[19] X. Wang, H. Li, Q. Ju, Q. Zhu, and F. Kong, Chem. Phys. Lett. **208**, 290 (1993).

[20] B. D. Green, G. E. Caledonia, R. E. Murphy, and F. X. Robert, J. Chem. Phys. **76**, 2441 (1982).

[21] P. Pechukas and J. C. Light, J. Chem. Phys. **42**, 3281 (1965).

[22] X. Wang, H. Li, Q. Zhu, F. Kong, and H. Yu, J. Chin. Chem. Soc. (Taipei) **42**, 399 (1995).

[23] For the $X\,^2\Pi$ state, C. Amiot, J. Mol. Spectrosc. **94**, 150 (1982); for the $A\,^2\Sigma^+$ state, J. Danielak, U. Domin, R. Kepa, M. Rytel, and M. Zachwieja, *ibid.* **181**, 394 (1997); for the $B\,^2\Pi$ state, R. Engleman, Jr. and P. E. Rouse, *ibid.* **37**, 240 (1971).

[24] L. G. Piper, T. R. Tucker, and W. P. Cummings, J. Chem. Phys. **94**, 7667 (1991); J. Luque and D. R. Crosley, J. Quant. Spectrosc. Radiat. Transf. **53**, 189 (1995).

[25] M. Bixon and J. Jortner, J. Chem. Phys. **48**, 715 (1968).

[26] H. Tsurumaki, Y. Fujimura, and O. Kajimoto, J. Chem. Phys. (in press).

[27] M. S. Child and R. T. Lawton, Faraday Discuss. Chem. Soc. **71**, 273 (1981); M. S. Child and L. Halonen, Adv. Chem. Phys. **57**, 1 (1984).

[28] A. L. L. East, A. R. W. McKellar, and J. K. G. Watson, J. Chem. Phys. **109**, 4378 (1998).

[29] H. Akagi, Y. Fujimura, and O. Kajimoto, J. Chem. Phys. **110**, 7264 (1999).